

MULTI-SCALE, MULTI-LEVEL, HETEROGENEOUS FEATURES EXTRACTION AND CLASSIFICATION OF VOLUMETRIC MEDICAL IMAGES

Shuai Li¹ Qinqing Zhao¹ Shengfa Wang² Aimin Hao¹ Hong Qin²

¹ State Key Laboratory of Virtual Reality Technology and Systems, Beihang University, China

² Department of Computer Science, Stony Brook University, USA

ABSTRACT

This paper articulates a novel method for the heterogeneous feature extraction and classification directly on volumetric images, which covers multi-scale point feature, multi-scale surface feature, multi-level curve feature, and blob feature. To tackle the challenge of complex volumetric inner structure and diverse feature forms, our technical solution hinges upon the integrated approach of locally-defined diffusion tensor (DT), DT-based anisotropic convolution kernel (DACK), DACK-based multi-scale analysis, and DT-governed curve feature growing. The extracted structural features can be further semantically classified. At the computational fronts, we design CUDA-based algorithm to conduct parallel computation for time consuming tasks. Various experiments and timing tests demonstrate the effectiveness, robustness, and high performance of our method.

Index Terms— Volumetric image, Multi-scale heterogeneous features, Curve propagation, Diffusion tensor, CUDA.

1. INTRODUCTION AND MOTIVATION

High-resolution medical volumetric image gives rise to a huge challenge for medical practitioners to focus on certain structural aspects. Although a variety of SIFT-like point feature extraction algorithms have become standard out-of-the-box tools in feature-driven registration, tissue segmentation, object recognition, and image fusion, heterogeneous structural features can better transform the difficult problem of understanding a raw data set into a simpler problem of analyzing a collection of meaningful feature elements, for example, blood vessels, bone cortices, and nodules can respectively be characterized by curve-like, surface-like, and blob-like features.

However, since volumetric images, especially for medical volumetric images, typically have much more complex inner structure and the diverse features may scatter apart over non-manifold volumetric geometry, the embedded structures usually have certain thickness, the definition of their heterogeneous structural feature is highly subjective and very difficult

to express. Meanwhile, naive feature extraction might obtain a large number of spurious small-scale structures, while user is generally only interested in a small fraction of some primary structures, thus quantitative refinement criteria with explicit physical meaning are also non-trivial problems. Besides, the overall performance of feature extraction and classification largely depends on the quality of the feature measurements, noisy extent, and the original data size. Thus, a unified and robust framework together with parallelly accelerated computation is urgently needed.

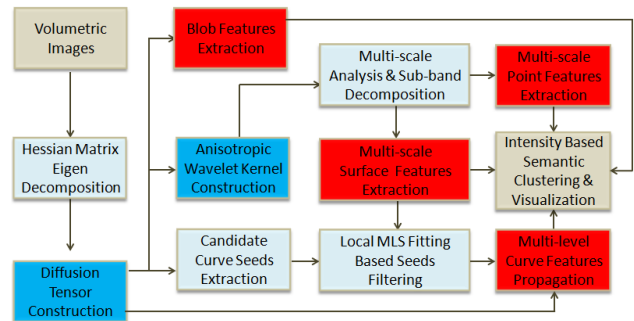


Fig. 1. The algorithmic architecture.

To tackle the aforementioned challenges, Fig. 1 illustrates the pipeline of our approach, where the salient contributions include:

(1) We devise a systematic and robust algorithm for semi-automatic heterogeneous structural feature extraction, classification, filtering and visualization, which requires no additional manual inputs except for a few threshold parameters.

(2) We define a diffusion tensor to facilitate the recognition of candidate curve seeds and blob features, guide CUDA-based global propagation of curve feature.

(3) We design a diffusion tensor based anisotropic convolution kernel to govern multi-scale point and surface feature extraction.

(4) We propose a projection distance based verification technique to exclude the false-alarm candidate curve seeds.

This research is supported by National Natural Science Foundation of China (No.61190121 and No.61190125) and NSF grants IIS-0949467, IIS-1047715, and IIS-1049448.

2. RELATED WORK

Monga et al. [1] first introduced crest lines by using image partial derivatives. Sato et al. [2] designed 3D filters to enhance the specific local 3D structures for tissue classification. However, their method often involves trials and errors due to the empirical criteria for filter selection. Bajaj et al. [3] proposed gradient vector diffusion based techniques for volumetric boundary extraction and visualization. Their work can produce reasonable results but sensitive to noise. Kindlmann et al. [4] extracted anisotropic crease from DTI image by extending marching cube method, but never demonstrated other geometric structures. Tricoche et al. [5] studied invariant crease lines in tensor space to detect the white matter structures of brain images. However, structures at significantly small or large scales are poorly detected. Schultz et al. [6] identified grid edges that are intersected by the extremal surfaces, and connected the intersection points to form curves or surfaces. The method is restricted to a uniform cubic grid, and does not guarantee the preservation of sharp surface features. Lempitzky [7] extracted separate iso-surfaces by replacing the original binary volume with a continuous-valued embedding function. It obtains smooth separating surface with fewer artifacts. Liu et al. [8] introduced a texture feature extraction method based on the spatial distribution patterns in volumetric neurological images. Barakat et al. [9] extracted high-quality crease surfaces by combining a front propagation strategy with a carefully managed parallel computation framework.

Although most of the above algorithms are competitive, they are rather lonesome. In sharp contrast to the existing work that concentrates on particular feature extraction, We have extracted multi-type structural feature on geometric surface mesh by introducing anisotropic diffusion tensor based voting scheme [10, 11]. Inspired by this, we fully extend the idea to handle multi-type, multi-scale, multi-level structure features directly on topology-free volumetric images.

3. DIFFUSION TENSOR AND ANISOTROPIC CONVOLUTION KERNEL

3.1. Hessian Eigen-system based Diffusion Tensor

Hessian matrix \mathbf{H} can fully grasp the second-order differential property, whose eigenvectors point to the directions of the principal curvatures and the eigenvalues correspond to the curvatures along those directions. For a unit vector \mathbf{n} , $A(p) = \mathbf{n}^T \mathbf{H}(p) \mathbf{n}$ measures the change rate along \mathbf{n} , which is maximum when \mathbf{n} is in the direction of the eigenvector corresponding to the largest eigenvalue of $\mathbf{H}(p)$. We construct an anisotropic diffusion tensor (DT) by factorizing \mathbf{H} with its eigenvalues ($\lambda_1 \geq \lambda_2 \geq \lambda_3 \geq 0$) and corresponding eigenvectors \mathbf{e}_k :

$$\mathbf{D}(p) = \tilde{\lambda}_1 \mathbf{e}_1 \mathbf{e}_1^T + \tilde{\lambda}_2 \mathbf{e}_2 \mathbf{e}_2^T + \tilde{\lambda}_3 \mathbf{e}_3 \mathbf{e}_3^T, \quad (1)$$

$$\tilde{\lambda}_i = \exp\left(-\frac{\lambda_i}{\sigma_d}\right), i = 1, 2, 3, \quad (2)$$

Diffusion parameter σ_d controls the diffusion velocities. DT is equal to construct an ellipsoid at each voxel to represent the direction and velocity of diffusion. According to the theory of Rayleigh quotient, the diffusion velocity from p along \mathbf{e} can be viewed as the length of the vector projected onto the ellipsoid, which is expressed as

$$vel(p, \mathbf{e}) = \frac{\mathbf{e}^T \mathbf{D}(p) \mathbf{e}}{\mathbf{e}^T \mathbf{e}}. \quad (3)$$

3.2. DT Space based Anisotropic Convolution Kernel

We derive DACK from the diffusion tensor and bilateral filter kernel. Since the surfaces and boundaries in volumetric images still have various directions due to their intrinsic geometrical structure, we devise a directional anisotropic convolution kernel by introducing the distance metric in diffusion tensor space. Given two neighboring voxels located at p and q , we first define their distance in DT space as

$$d_D(p, q) = \exp(-(p - q)^T (w_{pq}(\mathbf{D}(p) + \mathbf{D}(q))^{-1} (p - q))), \quad (4)$$

w_{pq} is introduced to amend the gradient, which changes in response to the intensity change of the neighboring voxels. $\mathbf{D}(p) + \mathbf{D}(q)$ describes the diffusivity and controls the diffusion directions and velocities. Then, we can define the DACK as

$$\Psi(p) = \frac{1}{W_p} \sum_{q \in N(p)} G_{\sigma_s}(p - q) G_{\sigma_k}(d_D(p, q)) I(q). \quad (5)$$

σ_k is a control parameter, which is set to the inverse of the maximal eigenvalues of diffusion tensors $\mathbf{D}(p)$ and $\mathbf{D}(q)$.

4. FEATURE EXTRACTION AND CLASSIFICATION

4.1. Multi-scale Point Features and Surface Features

Multi-scale analysis allows studying the multi-scale structure of volumetric images. We adopt dyadic wavelet transform to conduct DACK-based multi-scale analysis by

$$I^{n+1}(p, \sigma_s) = \frac{1}{W_p} \sum_{q \in N(q)} \omega^n(p - q, \sigma_s) G_{\sigma_k}(d_D^n(p, q)) I^n(q), \quad (6)$$

$$\omega^n(x, \sigma_s) = \begin{cases} G_{\sigma_s}(\|\frac{x}{2^n}\|) & \text{if } \frac{x}{2^n} \in Z^3 \text{ and } \|\frac{x}{2^n}\| < m \\ 0 & \text{otherwise} \end{cases} \quad (7)$$

where n represents the n -th scale level, m is a threshold to control the size of neighboring region. To improve computation efficiency, we update $d_D^n(p, q)$ only in response to the

change of w_{pq} while preserving $\mathbf{D}(p) + \mathbf{D}(q)$ according to Eq. (4). After $k + 1$ iterations, the approximate subband corresponding to a certain scale can be obtained, and k detail subbands are respectively the difference between the neighboring approximate subband. It is exactly an anisotropic approximation to the Laplacian. Thus, multi-scale point features can be obtained by extracting local minima/maxima from the detail subbands across scales. An example is shown in Fig. 6B, where the larger point means it is significant in a larger scale.

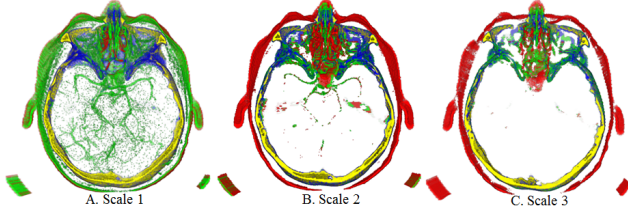


Fig. 2. Multi-scale surface features.

Surface features can also exist at various scales with different levels of details. In common sense the highest frequency details usually correspond to finest scale features while lower frequency corresponds to coarser scale features. With no additional computation cost, we can obtain the multi-scale surface features directly from the decomposed detail subbands. For a larger n , each individual voxel will contribute less to the surface variation and high-frequency oscillations will be attenuated, which is analogous to a low-pass filter. Besides, the original intensity of volumetric images can provide enough information to discriminate different materials, thus we employ adaptive K-means algorithm to conduct semantic classification. Fig. 2 illustrates the semantic classification results of the geometrically similar multi-scale surface features, where the adaptively determined cluster number K is 4.

4.2. Blob Feature and Multi-level Curve Feature

We conduct DT eigen-values analysis to classify voxels into blobs, candidate curve seeds, and noise. To separate features without any ambiguity, we design a criterion according to the characteristics of the normalized eigen-values ($\bar{\lambda}_i$). **Blob:** $\bar{\lambda}_1$, $\bar{\lambda}_2$, and $\bar{\lambda}_3$ are equally dominant (> 0.6); **Candidate curve seed:** $\bar{\lambda}_3$ is dominant (> 0.6), $\bar{\lambda}_1$ and $\bar{\lambda}_2$ are close to 0; **Noise:** $\bar{\lambda}_1$, $\bar{\lambda}_2$, and $\bar{\lambda}_3$ are close to 0, and its principal diffusion directions are different from its neighboring voxels. As the blob features shown in Fig. 6E, we then adopt the same clustering algorithm to further conduct semantic classification.

As shown in Fig. 3A, some of the candidate curve seeds may be false-alarm due to the jagged boundary voxels, whose projection distance to the locally fitted surface will be relatively larger than the jagged voxels. Thus, we can effectively filter out these false-alarm curve seeds according to the pro-

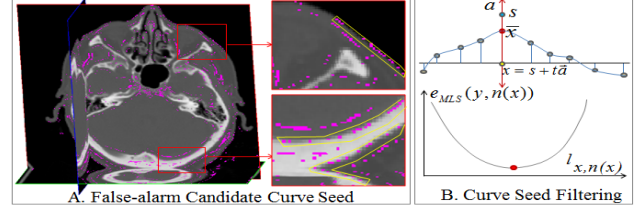


Fig. 3. Illustration of false-alarm curve seeds filtering.

jection distance to local fitted surface by minimizing the following energy function:

$$e_{MLS}(x, a) = \sum_{p_i \in P} (\langle a, p_i \rangle - \langle a, x \rangle)^2 \theta(x, p_i), \quad (8)$$

As shown in Fig. 3B, \vec{a} is the normal of the plane which is passed through by the point $x = s + t\vec{a}$, t is the distance from s to the plane, and $\theta(x, p_i) = e^{-\frac{(x-p_i)^2}{h^2}}$ is the Gaussian function. Let $l_{x,n(x)}$ be the line passing through x with direction $n(x) = \text{argmin}_a e_{MLS}(x, a)$, the surface is formed by points x , and x satisfies $x \in \text{arglocalmin}_{y \in l_{x,n(x)}} e_{MLS}(y, n(x))$.

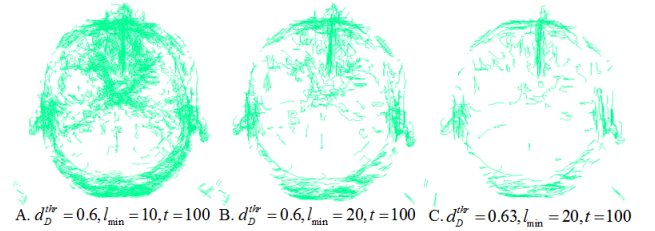


Fig. 4. Multi-level curve features. The parameter d_D^{thr} is a threshold value which controls the significant level of the curve feature, while the parameter l_{min} limits the length of the extracted curves.

Based on the filtered curve seed set, the curve features can be obtained through CUDA-based parallel propagation governed by diffusion tensor, which can be defined as

$$\begin{cases} c(v, t+1) = \text{argmax}_q d_D(c(v, t), q), & q \in \Omega_{c(v,t)} \\ \text{and } d_D(c(v, t), q) > d_D^{thr}, \\ c(v, 0) = v, & v \in S_f, \\ c(v, 0) = 0, & v \in \text{others}, \end{cases} \quad (9)$$

t means iterative propagation, $v \in \mathbb{R}^3$ represents the voxel position, Ω_v is the one-ring neighboring voxel set, d_D^{thr} is a threshold that controls the significant level of the curve feature, and the larger d_D^{thr} will result in the extraction of sharper curve features. Besides, no matter how empirically fine-tuning the parameter d_D^{thr} , some small curve features

may still occur, which makes the results rather chaotic. It is necessary to filter out the spurious small curves, which can be achieved by using another threshold parameter l_{min} to limit the arc-length of extracted curves. By fine-tuning the parameters d_D^{thr} and l_{min} , we can extract multi-level curve features, and Fig. 4 shows some examples resulted from different combinations of these two parameters.

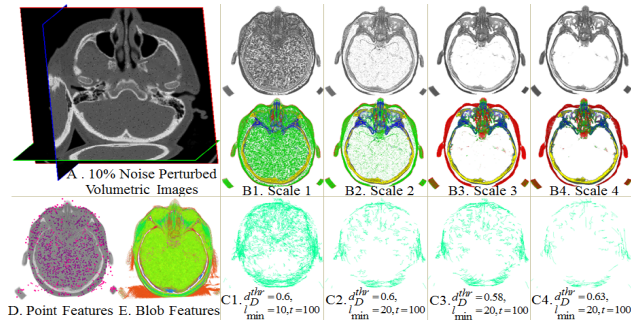


Fig. 5. Multi-scale heterogeneous features in 10% noise-perturbed MRI head images. By tuning the parameters d_D^{thr} and l_{min} , it can extract multi-level curve features, and the larger the d_D^{thr} leads to the sharper curve features.

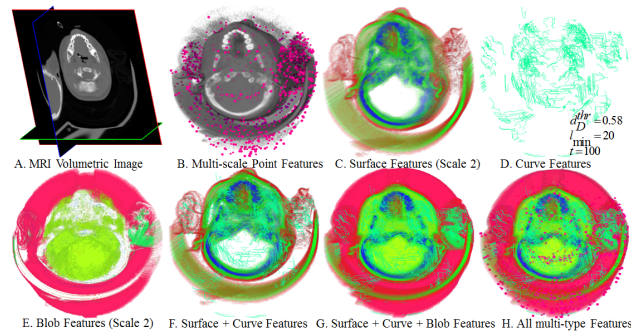


Fig. 6. Heterogeneous features in MRI baby head images.

5. EXPERIMENTAL RESULTS

Our prototype system is implemented using C++ and CUDA. We conduct all the experiments on a commodity laptop with NVIDIA GeForce 330M GPU, Intel Core (TM) i7 CPU (1.6GHz, 2 cores) and 4G RAM.

To examine the robustness of our method, we perturb the original image with 10% (of average intensity) random noise (Fig. 5A). Fig. 5B1 to Fig. 5B4 demonstrate the multi-scale surface features, comparing with Fig. 2, our method can almost obtain the same results when the scales are a bit larger

(e.g., B3 and B4). Fig. 5C1 to Fig. 5C4 show the extracted multi-level curve features with the same input parameters as Fig. 4, where all the important curves that naturally depict the global structures are correctly extracted and retained. Besides, Fig. 5E correctly removes the noisy points and illustrates the classification result for blob features. Therefore, our method proves to be robust to noise. Additionally, we conduct experiments on some other volumetric datasets. Fig. 6 shows the heterogeneous feature classification results of MRI baby head volume. Since the classification for each type of heterogeneous features is further conducted based on the extracted features, it will split or merge some features according to their respective classification criteria, for example, the classification number of blob feature in Fig. 6 appears different from that of the surface feature.

Table 1. Time testing (in seconds) of experiments.

Image Size	DTC	DACKD	MSE	BFCSE	CFPF
$256^2 \cdot 73$	4.8	30.3	84.2	85.4	9.2
$256^2 \cdot 73$	4.9	36.9	77.1	96.6	12.8
$256^2 \cdot 78$	9.4	34.8	86.6	78.4	6.8
$256^2 \cdot 62$	4.1	27.7	56.8	79.5	16.7
$256^2 \cdot 62$	4.2	26.5	62.2	60.2	5.1

Table 1 documents the time testing results, including CUDA-based DT construction (DTC), DACK based multi-scale decomposition (DACKD), multi-scale surface extraction (MSE), blob feature and curve seed extraction (BFCSE), and CUDA-based curve feature propagation and filtering (CFPF) with 100 iterations. Benefiting from CUDA, conventional time-consuming steps, such as DTC and CFPF, have gained remarkable performance speedup, which only costs about 10 seconds. Thus, our method can be used to enhance mission-critical processing of patient-specific images.

6. CONCLUSION AND FUTURE WORK

In this paper, we have detailed a comprehensive heterogeneous feature extraction and classification method for volumetric medical images. The technical novelty is centered on Hessian eigen-system based DT, DT assisted multi-scale analysis, DT governed curve propagation, and CUDA-accelerated parallel computation. Extensive experiments and time testing state that our method has superior performance in time efficiency, robustness, and functional integration.

$$\bar{d} = \frac{1}{k} \sum_{i=1}^k d_i$$

Our ongoing efforts are geared towards applying this approach to volumetric image vectorization, material-sensitive finite element meshing, and feature-driven illustrative visualization. Moreover, extending the key idea to handle diverse data types, such as volumetric medical vector/tensor images, point clouds, and higher dimensional manifolds in scientific disciplines also deserves further investigation.

7. REFERENCES

- [1] O. Monga and S. Benayoun, "Using partial derivatives of 3d images to extract typical surface features," *Computer Vision and Image Understanding*, vol. 61, pp. 171–189, 1995.
- [2] Y. Sato, C. F. Westin, A. Bhalerao, S. Nakajima, N. Shiraga, S. Tamura, and R. Kikinis, "Tissue classification based on 3d local intensity structures for volume rendering," *IEEE Transactions on Visualization and Computer Graphics*, vol. 6, pp. 160–180, 2000.
- [3] C. Bajaj, Z.-Y. Yu, and M. Auer, "Volumetric feature extraction and visualization of tomographic molecular imaging," *Journal of Structural Biology*, vol. 144, pp. 132–143, 2003.
- [4] G. L. Kindlmann, X. Tricoche, and C.-F. Westin, "Delineating white matter structure in diffusion tensor mri with anisotropy creases," *Medical Image Analysis*, vol. 11, no. 5, pp. 492–502, 2007.
- [5] X. Tricoche, G. Kindlmann, and C.-F. Westin, "Invariant crease lines for topological and structural analysis of tensor fields," *IEEE Transactions on Visualization and Computer Graphics*, vol. 14, no. 6, pp. 1627–1634, 2008.
- [6] T. Schultz, H. Theisel, and H.-P. Seidel, "Crease surfaces: From theory to extraction and application to diffusion tensor mri," *IEEE Transactions on Visualization and Computer Graphics*, vol. 16, pp. 109–119, 2010.
- [7] V. Lempitsky, "Surface extraction from binary volumes with higher-order smoothness," in *Computer Vision and Pattern Recognition*, 2010, pp. 1197–1204.
- [8] S.-d. Liu, W.-D. Cai, L.-F. Wen, S. Eberl, M.J. Fulham, and D.-G. Feng, "A robust volumetric feature extraction approach for 3d neuroimaging retrieval," in *Engineering in Medicine and Biology Society*, 2010, pp. 5657–5660.
- [9] S. Barakat, N. Andryscio, and X. Tricoche, "Fast extraction of high-quality crease surfaces for visual analysis," *Computer Graphics Forum*, vol. 30, no. 3, pp. 961–970, 2011.
- [10] S.-F. Wang, T.-B. Hou, Z.-X. Su, and H. Qin, "Diffusion tensor weighted harmonic fields for feature classification," in *Pacific Graphics*, 2011, pp. 93–98.
- [11] S.-F. Wang, T.-B. Hou, S. Li, Z.-X. Su, and H. Qin, "Anisotropic elliptic pdes for feature classification," *IEEE Transactions on Visualization and Computer Graphics*, to appear, 2013.